THE JOURNAL OF NAVIGATION (2014), **67**, 711–725.
doi:10.1017/S0373463314000204

A New Approach to Calculate the Vertical Protection Level in A-RAIM

Yiping Jiang and Jinling Wang

(*School of Civil and Environmental Engineering University of New South Wales, Sydney, Australia*)
(E-mail: yiping.jiang@student.unsw.edu.au)

Four methods to calculate the Vertical Protection Level (VPL) can be used in Advanced Receiver Autonomous Integrity Monitoring (A-RAIM), among which the ideal method is the strictest one. To obtain the ideal VPL satisfying the exact required integrity risk, the worst case bias with the maximum integrity risk is searched for. This investigation has found that the correct worst case highly depends on the choice of the input VPL. To gain the correct result, the computation becomes complex and the accuracy of the result is compromised. Therefore, a new procedure is designed with a new search: the maximum VPL is searched to encompass all possible bias sizes. Since VPL is calculated with a given integrity risk for each bias size, the uncertainty of the arbitrary VPL input in the ideal method is avoided. Also, an optimisation algorithm is adopted to improve computational efficiency. It is shown that the new method is more reliable and efficient than the current best method. Simulation results worldwide also show that the new approach has improved A-RAIM availability from 32%–38% to 74% with GPS and from 44%–43% to 85% with Galileo.

KEYWORDS

1. RAIM. 2. GNSS. 3. Multiple Hypothesis. 4. Solution Separation. 5. Classic RAIM.

Submitted: 12 September 2013. Accepted: 24 February 2014. First published online: 9 April 2014.

1. INTRODUCTION. Receiver Autonomous Integrity Monitoring (RAIM) was proposed to provide a navigation solution with guaranteed integrity using methods of consistency checking among measurements within a Global Positioning System (GPS) receiver (Brown, 1992; Lee, 1986). Its functions include the calculation of protection level and fault detection (Wang and Ober, 2009). The purpose is to produce an upper bound that is not exceeded with given risks. The protection level is compared with an alert limit to decide the availability so that users are aware of any hazardous situation when no alarm is generated but the position error is larger than allowed. With the advent of next-generation Global Navigation Satellite Systems (GNSS) and augmentation systems, A-RAIM, a new integrity monitoring architecture, is under study where the burden of integrity monitoring among space-based and ground-based augmentation systems and aircraft receivers is adjusted. The purpose is to provide the Localiser with the Vertical Guidance-200 (LPV-200) service worldwide

through to 2020 (GEAS, 2008; 2010). Two current methods that can be adopted for calculation of VPL in A-RAIM were studied and compared by Jiang and Wang (2014). VPL is then compared with Vertical Alarm Limit (VAL) as one of the conditions to decide service availability. However, the application of other methods to calculate VPL for this framework is very limited. Efforts are made in this study to integrate all popular methods in this framework with the focus to propose a new approach to improve A-RAIM availability.

When calculating the VPL with the conventional algorithms, there are mainly three options: the classic method (Brown and Chin, 1998), the method in Walter and Enge (1995) and the solution separation method (Brenner, 1996). There are also different ways to fix the size of the unknown bias for calculation of VPL (Ober, 2003): Minimal Detectable Bias (MDB), Minimal Hazardous Bias (MHB) and Worst Case Bias (WCB). The MDB is used in the classic method. The WCB has been used to derive the ideal VPL with the exact value of VPL satisfying the required integrity risk (Milner and Ochieng, 2011), which is also applied in A-RAIM (Milner and Ochieng, 2010). The WCB that produces the maximum integrity risk is searched within the range of MHB and MDB. However, to ensure the maximum integrity risk value is the same as the given one, the input VPL also needs to be searched. With two search loops, the calculation is complex and the accuracy is not guaranteed. A new procedure to calculate the exact VPL value is presented to overcome this problem with the following procedure. First, the search range is defined in the domain of Type II error, which has a one-to-one relationship with the bias size with a given Type I error. Then the VPL corresponding to each Type II error in the search domain is calculated. The maximum VPL is the result that is able to protect the user against all possible bias. Also, an optimisation algorithm is adopted to reduced the computational time.

All the methods to calculate VPL are incorporated in the A-RAIM structure, where the multiple hypothesis structure in the Multiple Hypothesis Solution Separation (MHSS) method (Pervan et al., 1998; Blanch et al., 2007; 2010) is an essential part. The advantages of the multiple hypothesis structure include a) the ability to accommodate a complete set of failure modes; b) the flexibility of risk allocation onto each hypothesis; c) flexibility to define the prior probability of any fault mode according to the environment.

The structure of this paper is as follows. In Section 2, the basic model is given and followed by the solution separation statistic used in A-RAIM. The equivalence of this statistic with other fault detection statistics is obtained. The allocation of integrity risk and continuity risk for A-RAIM is shown in Section 3. In Section 4, three different methods for the calculation of VPL are provided. The design process of the new approach to calculate the ideal VPL is described in Section 5. A numerical example to illustrate the mechanism is shown in Section 6. Under a given error model, the risk definition and constellation and the A-RAIM performances are provided in Section 7.

2. SYSTEM MODELS AND TEST STATISTICS.

The mathematical and stochastic models to relate measurements to the position solution after linearization are

$$E(y) = Ax;\ D(y) = Q_y = P^{-1} \tag{1}$$

https://doi.org/10.1017/S0373463314000204 Published online by Cambridge University Press

where $y \in R^{n\times 1}$ is the measurement vector, $x \in R^{n\times 1}$ is the unknown position vector, $A \in R^{m\times n}$ is the design matrix with rank n and $Q_y \in R^{m\times m}$ is the positive definite covariance matrix of the measurements.

The vertical position estimation $\hat{x}_v$ is,

$$\hat{x}_v = e_v^T (A^T P A)^{-1} A^T P y \tag{2}$$

where $e_v \in R^{n\times 1}$ is a zero vector with the third element as one.

The vertical position error is the difference between $\hat{x}_v$ and the true vertical position x_v,

$$\nabla x_v = \hat{x}_v - x_v \tag{3}$$

The test statistic used in A-RAIM is the solution separation (GEAS, 2010). The subset vertical position estimation $\hat{x}_{vi}$ is the weighted least squares estimation with the ith measurement removed. The solution separation is $\hat{x}_v - \hat{x}_{vi}$. The standardized solution separation is used as the test statistic for failure mode i,

$$t_i = \frac{\hat{x}_v - \hat{x}_{vi}}{\sigma_{ss,i}} \tag{4}$$

where $\sigma_{ss,i}$ is the standard deviation of the solution separation and $\sigma_{ss,i} = \sqrt{\sigma_v^2 - \sigma_i^2}$ without correlation among measurements (Blanch et al., 2010) with σ_v as the standard deviation of the vertical position error ∇x_v and σ_i as the standard deviation of the vertical subset solution error $\nabla x_{vi} = \hat{x}_{vi} - x_v$.

The relationship between the solution separation statistic and other test statistics is not clearly defined (Young and McGraw, 2003). It is shown below that the equivalence exists without correlation. Assuming there is an unknown bias in the measurements, $\hat{x}_{vi}$ was proved to be equivalent with the unbiased vertical position estimation (Diggelen and Brown, 1994). Therefore it can be concluded that the test statistic in Equation (4) is equivalent with the "maximum residual" (Kelly, 1998) and the one in the data-snooping method (Baarda, 1967) when all the measurements are uncorrelated, which is the case for GNSS A-RAIM.

Also, the slope parameter $Vslope_i$ in the classic method (Brown and Chin, 1998), which is also defined as the project matrix from the test statistic domain to the position domain, was proved to be equivalent with $\sigma_{ss,i}$ (Blanch et al., 2010),

$$Vslope_i = \frac{|e_v^T (A^T P A)^{-1} A^T P e_i|}{\sqrt{e_i^T (P - PA(A^T P A)^{-1} A^T P) e_i}} = \sigma_{ss,i} \tag{5}$$

where $e_i \in R^{m\times 1}$ is a zero vector with the ith element as one.

3. ALLOCATION OF INTEGRITY RISK AND CONTINUITY RISK AMONG FAILURE MODES.

In A-RAIM, the integrity risk and continuity risk are defined to calculate VPLs. The integrity risk is the probability of the navigation system failing to protect against the hazardous situation within the Time-To-Alert (TTA), which is caused by faults producing undetected navigation errors greater than a VAL (GEAS, 2008; 2010). The total integrity risk IR is divided into the horizontal IR_h and vertical IR_v. Within the context of A-RAIM

https://doi.org/10.1017/S0373463314000204 Published online by Cambridge University Press

and LPV-200, the vertical integrity risk is then divided onto each failure mode. The vertical integrity risk under failure mode i IR_i is defined as (GEAS, 2008),

$$IR_i = P\{|\nabla x_v| > VPL \cap |t_i| < T_i|H_i\}P_{H_i} \tag{6}$$

where P_{H_i} is the prior probability of the failure mode i H_i. T_i is the threshold to be compared with the test statistic.

Without correlation among the multivariate normal distribution of the position error and test statistic, the independence of these two is concluded (Ober, 2003; Milner and Ochieng, 2010). Therefore, Equation (6) can be expressed as,

$$IR_i = P\{|\nabla x_v| > VPL|H_i\}P\{|t_i| < T_i|H_i\}P_{H_i} \tag{7}$$

Under failure mode i, the fault free hypothesis H_{i0} is tested against the hypothesis H_{ia} for the case of a faulty measurement. The corresponding integrity risk for the hypotheses are IR_{i0} and IR_{ia}. There are two types of test errors: probability of missed detection (P_{MD}) and probability of false alarm (P_{FA}). In A-RAIM, P_{MD} is not a given parameter and the P_{MD} under the faulty mode i is,

$$P_{MDi} = P\{|t_i| < T_i|H_{ia}\} \tag{8}$$

The continuity risk is defined as the probability of continuity break per 15 s for the duration of aircraft approach (GEAS, 2008). The P_{FA} can be obtained from the fault free continuity risk in A-RAIM (GEAS, 2008),

$$P_{FAi} = P\{|t_i| > T_i|H_{i0}\} \tag{9}$$

4. THREE METHODS TO CALCULATE VPLS FOR A-RAIM.

There is no unknown bias in both position error and the test statistic under fault free modes. With P_{FA} given in A-RAIM, Equation (9) is applied in Equation (7). The fault free VPL under H_{i0} is,

$$VPL_{i0} = K\left[1 - \frac{IR_{i0}}{2P_{H_{i0}}(1 - P_{FAi})}\right]\sigma_v \tag{10}$$

where $K[]$ is the inverse of the cumulative distribution function of a Gaussian random variable with zero mean and unit variance. In current methods, $1 - P_{FAi}$ is assumed to be one under the fault free mode.

Under the faulty mode, there is an unknown bias in both position error and test statistic, and the P_{MD} under the faulty mode is not given. Therefore, the straightforward derivation of VPL is impossible. Beside the ideal VPL (VPL_{MO}) (Milner and Ochieng, 2010) which aims to derive the exact solution, there are other algorithms used to obtain conservative VPLs with higher efficiency of computation, where the conservative VPL is able to guarantee a lower than given integrity risk. Three current algorithms adapted in the A-RAIM framework are listed below.

In Brown and Chin (1998), the bias is fixed with a given P_{FA} and integrity risk and the noise is bounded by another term (Angus, 2007). Therefore, the VPL_{BC} under each single hypothesis is

$$VPL_{BCi} = \delta_i \cdot Vslope_i + K\left(1 - \frac{IR_{ia}}{2P_{H_{ia}}}\right)\sigma_v \tag{11}$$

https://doi.org/10.1017/S0373463314000204 Published online by Cambridge University Press

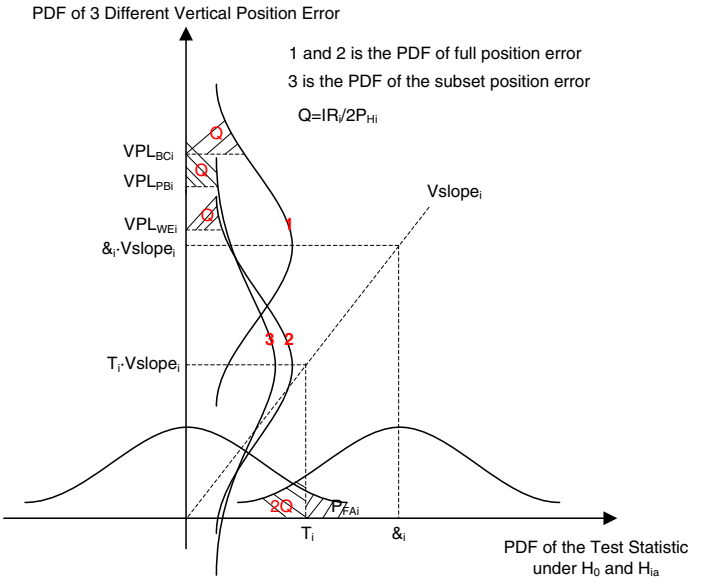

Figure 1. Three VPL Calculation Mechanisms.

Instead of the bias, the threshold is projected into the position domain in Walter and Enge (1995) which generates a smaller VPL (VPL_{WE}) than the one in Equation (11),

$$VPL_{WEi} = K\left(1 - \frac{P_{FAi}}{2}\right)Vslope_i + K\left(1 - \frac{IR_{ia}}{2P_{H_{ia}}}\right)\sigma_v \tag{12}$$

The total position error is separated into the solution separation and the subset position error without the necessity of projecting from the test statistic domain in Pervan et al. (1998); Blanch et al. (2010). And the VPL_{PB} under each single hypothesis is,

$$VPL_{PBi} = K\left(1 - \frac{P_{FAi}}{2}\right)\sigma_{ss,i} + K\left(1 - \frac{IR_{ia}}{2P_{H_{ia}}}\right)\sigma_i \tag{13}$$

These three different methods to calculate VPL are shown in Figure 1.

5. THE NEW APPROACH TO CALCULATE THE VPL IN A-RAIM.

The exact VPL value that is able to protect the user against all possible bias, with a given integrity risk value, is illustrated in Figure 2. What is worth noting here is the different P_{MD} in VPL_{BC} and the exact VPL, where the first one has a fixed value as derived by the given integrity risk $IR_{ia}/P_{H_{ia}}$, whereas the latter one needs to be searched for. A procedure was designed to calculate the ideal VPL in Milner and Ochieng (2010). In this section, the problems in the ideal VPL method are described, followed by the design process of the new procedure.

5.1. *The Design Process.* Since VPL and bias size are unknown under the faulty case in Equation (7), it is impossible to get a unique solution without a search of the worst case bias. The calculation of VPL_{MO} in Milner and Ochieng (2011) is designed with a worst case search: the WCB with maximized integrity risk

https://doi.org/10.1017/S0373463314000204 Published online by Cambridge University Press

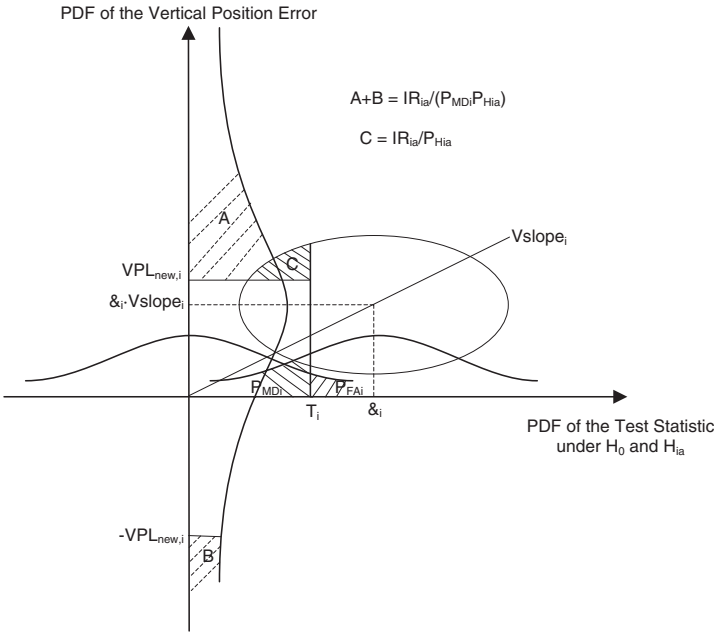

Figure 2. Illustration of the exact VPL.

is searched within the range of MHB and MDB. The ideal VPL that matches the exact required integrity risk is then calculated with the WCB. MHB is derived with $P\{|\nabla x_v| > VPL|H_{ia}\} = IR_{ia}/P_{H_{ia}}$ with an arbitrary VPL input. MDB is derived with $P\{|t_i| < T_i|H_{ia}\} = IR_{ia}/P_{H_{ia}}$. This procedure induces a problem: the correct WCB relies on correct choice of the input VPL used to derive MHB. If not, the resulting VPL does not correspond to the given integrity risk, causing safety outages. To avoid this and obtain the right VPL value with the given integrity risk, another search loop within a VPL range is added. Thus, the computation process becomes complex, and several conditions are designed to simplify the procedure.

An example in Figure 3 is used to show the situation when the input VPL is not properly chosen. The black horizontal line represents the given integrity risk which was used to derive the MHB and MDB. The integrity risk on the vertical axis in Equation (7) is calculated with the bias on the horizontal axis and the VPL_{MO} derived by the correct VPL input (red line) and the wrong VPL input (green line).

It is validated in Figure 3 with the red line that the maximum integrity risk within the bias range does correspond with the given integrity risk with the condition of a correct VPL input. Also the green line is an example when the given integrity risk is used to derive MHB and MDB, but with the wrong VPL input, the derived VPL_{MO} resulted in an integrity risk which is larger than the given one. Therefore another search loop of VPL is needed in this method.

To overcome this limitation, the following new procedure is proposed. Firstly, P_{MD} and the bias have a one-to-one relationship with the bias derived by P_{MD} and P_{FA} in Equations (8) and (9). When P_{MD} is larger, the bias is smaller. Therefore, the search boundary is defined in the P_{MD} domain to accommodate all possible bias size by using

https://doi.org/10.1017/S0373463314000204 Published online by Cambridge University Press

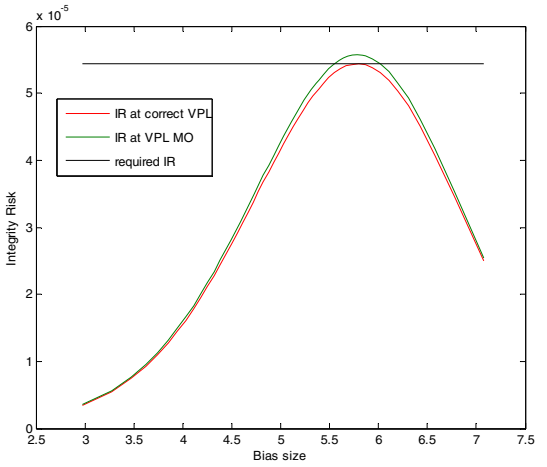

Figure 3. An Example of the wrong input VPL in VPL_{MO}.

all possible P_{MD} values. The boundary of the P_{MD} values for the bias/fault in the ith measurement is defined as follows,

$$\frac{IR_{ia}}{P_{H_{ia}}} < P_{MDi} < 1 \tag{14}$$

where the left side of the boundary is derived as

$$P_{MDi} = \frac{IR_{ia}/P_{H_{ia}}}{P\{|\nabla x_v| > VPL|H_{ia}\}} > \frac{IR_{ia}}{P_{H_{ia}}}.$$

This is based on the fact that with Equation (7), $0 < P\{|\nabla x_v| > VPL|H_{ia}\} < 1$, and at the same time, $IR_{ia}/P_{H_{ia}}$ is constant when the integrity risk to the fault in the ith measurement is allocated.

Based on Equation (14), the bias should satisfy

$$\delta_i < K\left(1 - \frac{P_{FAi}}{2}\right) + K\left(1 - \frac{IR_{ia}}{P_{H_{ia}}}\right) \tag{15}$$

The relationship between the P_{MD} and VPL with a given integrity risk is shown in Figure 4, and the relationship between the P_{MD} and the integrity risk with a given VPL is shown in Figure 5. P_{MD} is changed to the bias, and a similar relationship is shown in Figures 6 and 7. The input integrity risk in Figures 4 and 6 is derived by the input VPL value in Figures 5 and 7. The maximum P_{MD} depicted in Figures 4 and 5 and the maximum bias shown in Figures 6 and 7 are the same respectively. Therefore, the worst case is defined as the maximum VPL in the new procedure, which is equivalent with the maximum integrity risk in the original method. The integrity risk with the maximum VPL is guaranteed to be the same as the required one. In this way, the uncertainty of the input VPL is avoided.

There are two ways to calculate the new VPL (VPL_{new}). The first option is the search method. In this method, the P_{MD} range is divided by pre-defined total search steps. Within each step, the P_{MD} value is then determined, and the VPL values with given integrity risk are calculated. The maximum VPL is the desired result. The

https://doi.org/10.1017/S0373463314000204 Published online by Cambridge University Press

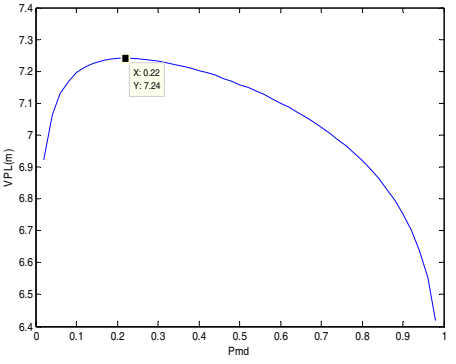

Figure 4. VPL as a function of P_{MD}.

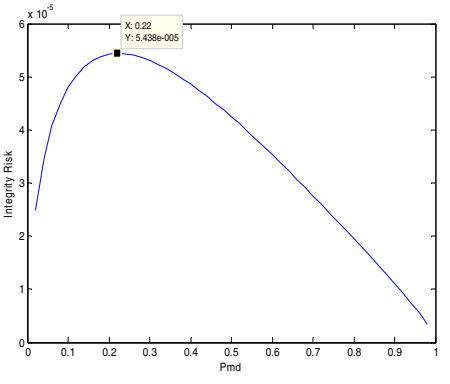

Figure 5. Integrity Risk as a function of P_{MD}.

criterion is described as,

$$\max(VPL),\ \text{subject to}\int_{-\infty}^{-\mathrm{VPL}} \mathrm{f(x)dx} + \int_{\mathrm{VPL}}^{+\infty} \mathrm{f(x)dx} = \frac{\mathrm{IR_{ia}}}{\mathrm{P_{H_{ia}} P_{MDi}}} \text{ and } \frac{\mathrm{IR_{ia}}}{\mathrm{P_{H_{ia}}}} < P_{\mathrm{MDi}} < 1 \tag{16}$$

where f(x) is the probability density function of $\tilde{x}_v$.

Although the search method is simplified with only one search loop, compared with the two loops of search for the $\mathrm{VPL_{MO}}$, the accuracy of the result is still not able to be controlled, depending on the total steps in the search loops. To gain results within the pre-defined accuracy, the analytical method is designed with an equivalent criterion to maximize the integrity risk as an inequality constrained maximization problem that can be solved by the optimization tool in MATLAB with the interior point method,

$$\begin{aligned} &\max_{\mathrm{VPL}}\left\{\mathrm{P_{MDi}}\left[\int_{-\infty}^{-\mathrm{VPL}} \mathrm{f(x)dx} + \int_{\mathrm{VPL}}^{+\infty} \mathrm{f(x)dx}\right]\right\}, \\ &\text{subject to}\int_{-\infty}^{-\mathrm{VPL}} \mathrm{f(x)dx} + \int_{\mathrm{VPL}}^{+\infty} \mathrm{f(x)dx} = \frac{\mathrm{IR_{ia}}}{\mathrm{P_{H_{ia}} P_{MDi}}} \text{ and } \frac{\mathrm{IR_{ia}}}{\mathrm{P_{H_{ia}}}} < P_{\mathrm{MDi}} < 1 \end{aligned} \tag{17}$$

https://doi.org/10.1017/S0373463314000204 Published online by Cambridge University Press

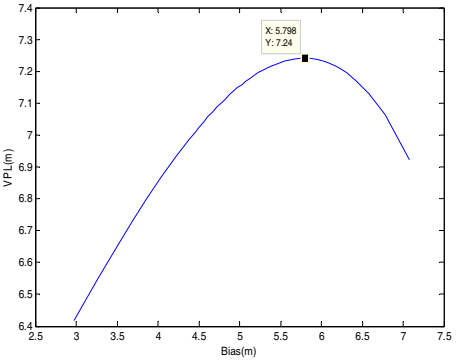

Figure 6. VPL as a function of Bias.

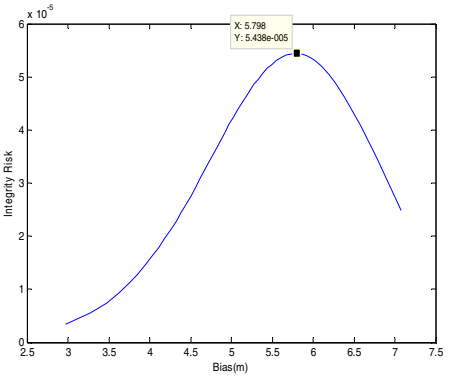

Figure 7. Integrity Risk as a function of Bias.

If convergent, the result derived from the analytical method should be within the pre-defined accuracy. The computation efficiency of both methods will be shown later by an example.

5.2. *Analysis of Conservativeness.* $\mathrm{VPL_{new}}$ as the exact value is compared with other VPLs to analyse the conservativeness. $\mathrm{VPL_{new}}$ can be expressed as a combination of the non-centrality part ∇x_i and the random part,

$$\mathrm{VPL_{new,i}} = \nabla \mathrm{VPL_i} + \mathrm{Q}\left(\nabla \mathrm{VPL_i}, \frac{\mathrm{IR_{ia}}}{\mathrm{P_{H_{ia}} P_{MDi}}}\right) \tag{18}$$

where the second parameter is the random part as a function of $\nabla \mathrm{VPL_i}$ and $\mathrm{IR_{ia}}/\mathrm{P_{H_{ia}} P_{MDi}}$ with Equations (16) or (17).

Based on Equation (14), the following inequality is derived,

$$\nabla \mathrm{VPL_i} < \left[K\left(1 - \frac{\mathrm{P_{FAi}}}{2}\right) + \mathrm{K}\left(1 - \frac{\mathrm{IR_{ia}}}{\mathrm{P_{H_{ia}}}}\right)\right] \mathrm{Vslope_i} \tag{19}$$

https://doi.org/10.1017/S0373463314000204 Published online by Cambridge University Press

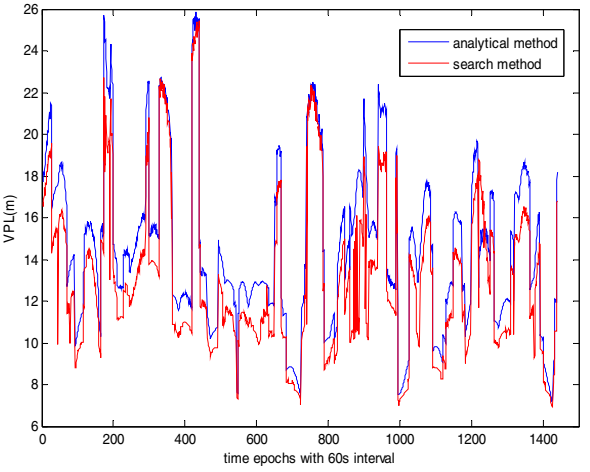

Figure 8. Two ways to calculate the VPL_{new}.

When $\nabla VPL_i \neq 0$, the following inequality is derived,

$$Q\left(\nabla VPL_i, \frac{IR_{ia}}{P_{H_{ia}} P_{MDi}}\right) < K\left(1 - \frac{IR_{ia}}{2P_{H_{ia}} P_{MDi}}\right)\sigma_v < K\left(1 - \frac{IR_{ia}}{2P_{H_{ia}}}\right)\sigma_v \tag{20}$$

Therefore, the conservativeness of the VPL_{BC} is obtained,

$$VPL_{new,i} < VPL_{BCi} \tag{21}$$

The position error can be regarded as a sum of two parts: solution separation and subset solution error,

$$|\nabla x_v| < |\hat{x}_v - \hat{x}_{vi}| + |\hat{x}_{vi} - x_v| \tag{22}$$

With the relationship of test statistic and solution separation in Equation (4), a given P_{MD} can be concluded

$$P\{|\hat{x}_v - \hat{x}_{vi}| < T_i \sigma_{ss,i} | H_{ia}\} = P_{MDi} \tag{23}$$

With Equation (7),

$$P\{|\hat{x}_{vi} - x_v| > VPL_{new,i} - T_i \sigma_{ss,i} | H_{ia}\} > \frac{IR_{ia}}{P_{H_{ia}} P_{MDi}} \tag{24}$$

Therefore,

$$VPL_{new,i} < K\left(1 - \frac{IR_{ia}}{2P_{H_{ia}} P_{MDi}}\right)\sigma_i + K\left(1 - \frac{P_{FAi}}{2}\right)\sigma_{ss,i} < VPL_{PBi} \tag{25}$$

Consequently, VPL_{BC} and VPL_{PB} are always conservative irrespective of the size of the bias.

6. A NUMERICAL EXAMPLE.

Results using measurements collected on UNSW campus within a 24-hour time span are shown in Figures 8 and 9. The mask angle of GPS was 5°. The prior probability for each local hypothesis is 1×10^{-5}.

https://doi.org/10.1017/S0373463314000204 Published online by Cambridge University Press

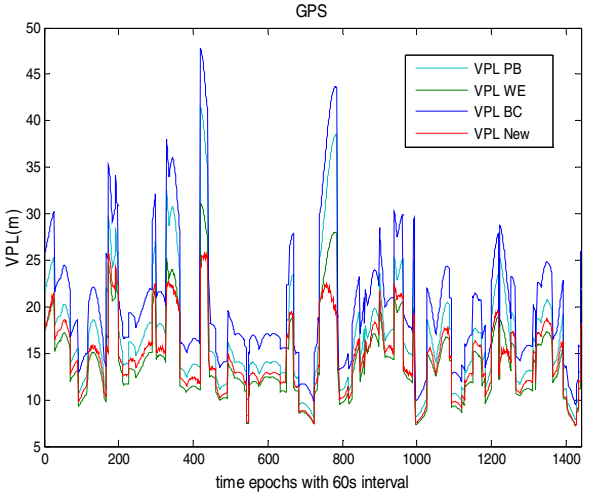

Figure 9. VPL_{new} and other VPLs.

The integrity risk under the fault free case is $4{\cdot}35\times10^{-8}$, and the same for the faulty case. The P_{FA} of each hypothesis is 4×10^{-6}. The measurements are assumed to follow standard normal distribution without correlation among each other. Two ways to calculate the new VPL, the search method given by Equation (16) and the analytical method given by Equation (17) where the accuracy of the integrity risk is set at 10^{-10}, are compared in Figure 8.

With the increase of the total number of the steps in the search method, the accuracy of the results increases. It was found that beyond around 150 steps there was no obvious accuracy increase so 150 steps were used. To ensure convergence in the analytical method, the initial value at epoch 1 was chosen by using the search method.

As demonstrated in Figure 8, the search method is not able to protect the user all the time, with the evidence that VPL from the search method is smaller than with the analytical one. This is caused by the accuracy problem within the search steps. Plus, the computation time for one epoch averages 5·26 s with 150 steps in the search method. Using the non-linear optimization tool in MATLAB, the analytical method can greatly improve the computation efficiency with an average of 0·35 s consumed for one epoch. Therefore, the analytical method should be used to determine VPL_{new} with higher computational efficiency and accuracy. The VPL_{new} determined by the analytical method together with other VPLs are shown in Figure 9.

VPL_{BC} and VPL_{PB} were always bigger than VPL_{new} with different levels of conservativeness, which is consistent with the proof in Section 5.2. There were situations where VPL_{WE} was smaller than VPL_{new} in this experiment, which is evidence that VPL_{WE} is not safe to be used. The computation time with the conventional methods (VPL_{PB} and VPL_{BC}) for one epoch averaged $1{\cdot}21\times10^{-3}$ s with the Intel Core 2 Duo Processor E8400. To gain the correct result of VPL_{MO} with 150 steps in the P_{MD} search and 500 steps in the VPL search within the range of $0\sim50$ m, it took an average of 9·32 s for one epoch.

https://doi.org/10.1017/S0373463314000204 Published online by Cambridge University Press

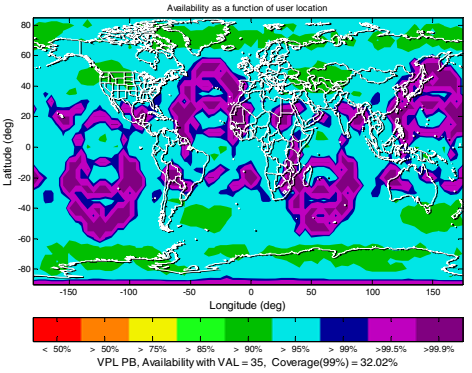

Figure 10. 99% Availability with VPL PB, 24GPS.

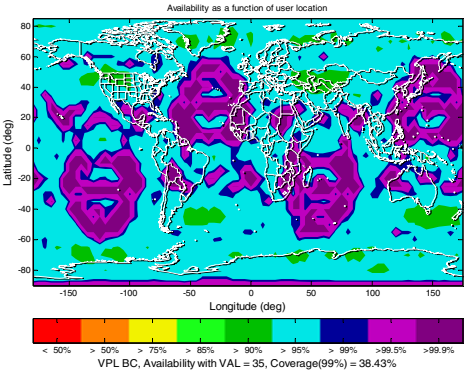

Figure 11. 99% Availability with VPL BC, 24GPS.

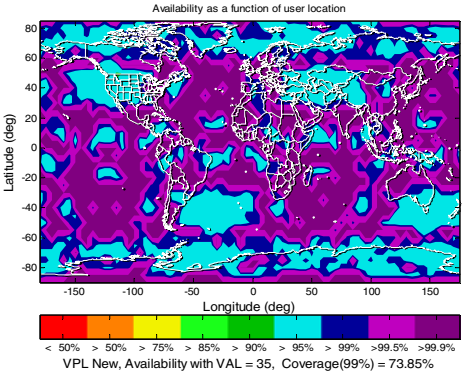

Figure 12. 99% Availability with New VPL, 24GPS.

7. A-RAIM PERFORMANCE. The simulation for A-RAIM was set up as follows to test the availability of LPV200. As the error model defined for this service, a bias term was added to gain more conservative results (GEAS, 2008; 2010). The values

https://doi.org/10.1017/S0373463314000204 Published online by Cambridge University Press

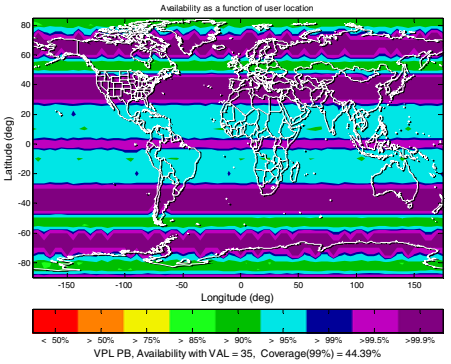

Figure 13. 99% Availability with VPL PB, 27Galileo.

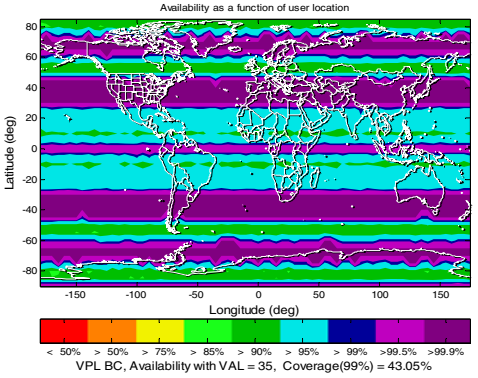

Figure 14. 99% Availability with VPL BC, 27Galileo.

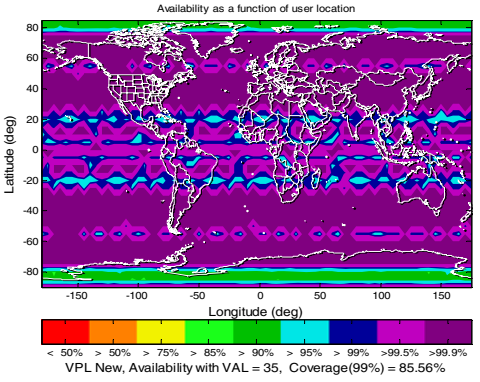

Figure 15. 99% Availability with New VPL, 27Galileo.

for the nominal bias and the maximum bias were 0·1 m and 0·75 m. The User Range Error (URE) and User Range Accuracy (URA) were 0·25 m and 0·5 m. The risk definition was defined as follows. The total integrity risk 2×10^{-7} was divided into the horizontal and vertical case evenly. Within the vertical case, the multiple fault modes

https://doi.org/10.1017/S0373463314000204 Published online by Cambridge University Press

were excluded, leaving the single fault and fault free hypotheses with the integrity risk as $8{\cdot}7\times10^{-8}$. The integrity risk was distributed evenly onto each hypothesis. The prior probability of each single fault mode was 1×10^{-5}. The probability of the null hypothesis was approximated as one. The continuity risk under the fault free and single fault modes was 4×10^{-6} separately. Again, the continuity risk was distributed evenly onto each hypothesis.

The almanac data for the standard 24 GPS and 27 Galileo satellite constellation was used to determine the geometry at each location with a $5\times5°$ grid on the world map at 50 m altitude. Results of VPL at each location were obtained every 6 minutes over the 24 hour duration. Mask angle of GPS and Galileo are 5° and 15° respectively. The availability was determined by comparing each VPL value with the VAL (35 m) for each location in one day. The percentage having over 99% availability over this time is shown worldwide. The simulation software is based on the MATLAB Algorithm Availability Simulation Tool (MAAST) provided by Stanford University. Simulation results are as follows.

It has been shown that A-RAIM performance is greatly improved using the new VPL with both GPS and Galileo. Also, $\mathrm{VPL_{PB}}$ showed worse results for A-RAIM performance than $\mathrm{VPL_{BC}}$ with GPS, but better performance with Galileo. Therefore, the relationship between $\mathrm{VPL_{PB}}$ and $\mathrm{VPL_{BC}}$ is dependent on geometry. It is also noted that the new VPL took around 100 times longer to calculate than the other two methods.

8. CONCLUDING REMARKS.

To gain the exact value with the required integrity risk, the new procedure is demonstrated to be simpler, more reliable and more computationally efficient than the current VPL methods. With conventional methods designed to gain the approximated values, A-RAIM performance is greatly improved with the new VPL method when compared with the conventional ones. While the computational burden is increased, the computation speed is sufficient for real-time applications. Also, two of the conventional methods, the classic method and the MHSS method, are proved to be safe regardless of the size of the bias, while the $\mathrm{VPL_{WE}}$ is not. With the optimization method given in the MATLAB toolbox, further efforts can be made to customize the optimization method for this specific problem to maximise the computational efficiency. In addition, the more complicated problem of computing exactly Horizontal Protection Level (HPL) should be further investigated in a separate study.

ACKNOWLEDGEMENTS

The first author is sponsored by the Chinese Scholarship Council for her PhD studies at the University of New South Wales, Australia.

REFERENCES

Angus, J.E. (2007). RAIM with Multiple Faults, *Navigation*, **53**(4), 249–257.

Baarda, W. (1967). *Statistical concepts in geodesy*. Netherlands Geodetic, Commission, Publications on Geodesy, New Series 2, No. 4, Delft, The Netherlands.

Blanch, J., Ene, A., Walter, T. and Enge, P. (2007). An Optimized Multiple Hypothesis RAIM Algorithm for Vertical Guidance, *ION GNSS 2007*, Fort Worth, TX.

Blanch, J., Walter, T. and Enge, P. (2010). RAIM with Optimal Integrity and Continuity Allocations under Multiple Failures, *IEEE Transactions on Aerospace and Electronic Systems*, **46**(3), 1235–1247.

Brenner, M. (1996). Integrated GPS/Inertial Fault Detection Availability, *Navigation*, **43**(2), 111–130.

Brown, R.G. (1992). A Baseline GPS RAIM Scheme and a Note on the Equivalence of Three RAIM Methods, NAVIGATION, *Journal of The Institute of Navigation*, Vol. **39**, No. 3, pp. 301–316.

Brown, R.G. and Chin, G.Y. (1998). Calculation of threshold and protection radius using chi-square methods-a geometric approach, *ION Red Books*.

Diggelen, F. and Brown, A. (1994). Mathematical aspects of GPS RAIM, *Position Location and Navigation Symposium, IEEE*, 733–738.

GEAS. (2008). *GNSS Evolutionary Architecture Study, GEAS Phase I* - Panel Report, FAA. http://www.faa.gov/about/office_org/headquarters_offices/ato/service_units/techops/navservices/gnss/library/documents/media/GEAS_PhaseI_report_FINAL_15Feb08.pdf.

GEAS. (2010). *GNSS Evolutionary Architecture Study, GEAS Phase II* - Panel Report, FAA. http://www.faa.gov/about/office_org/headquarters_offices/ato/service_units/techops/navservices/gnss/library/documents/media/GEASPhaseII_Final.pdf.

Jiang, Y. and Wang, J. (2014). A-RAIM and R-RAIM Performance with the Classic Method and the MHSS Method, *The Journal of Navigation*, **67**(1), 49–61.

Kelly, R. J. (1998). The linear model, RNP, and the near optimum fault detection and exclusion algorithm, Global Positioning System, Vol. V, *The US Institute of Navigation (ION)*, 227–259.

Lee, Y.C. (1986). Analysis of the Range and Position Comparison Methods as Integrity in the User Receiver, Proceedings of the Annual Meeting of the ION, Seattle, WA.

Milner, C. and Ochieng, W. (2010). ARAIM for LPV-200: The Ideal Protection Level, *Proceedings of the 23rd ION GNSS 2010*, Portland, OR, pp. 3191–3198.

Milner, C. and Ochieng, W. (2011). Weighted RAIM for APV: The Ideal Protection Level, *The Journal of Navigation*, **64**, 61–73.

Ober, P.B. (2003). *Integrity Prediction and Monitoring of Navigation Systems*. PhD Thesis. TU Delft.

Pervan, B., Pullen, S. and Christie, J. (1998). A Multiple Hypothesis Approach to Satellite Navigation Integrity, *Journal of the Institute of Navigation*, **45**(1), 61–84.

Walter, T. and Enge, P. (1995) Weighted RAIM for Precision Approach, *Proceedings of ION GPS-95*, Palm Springs, CA, pp. 1995–2004.

Young, R.S.Y. and McGraw, G.A. (2003). Fault Detection and Exclusion Using Normalized Solution Separation and Residual Monitoring Methods, *NAVIGATION*, **50**(3): 151–170.

Wang, J. and Ober, P.B. (2009). On the Availability of Fault Detection and Exclusion in GNSS Receiver Autonomous Integrity Monitoring, *the Journal of Navigation*, **62**(2), 251–261.